Blind deconvolution under band limitation

Noriaki MIURA

Department of Computer Sciences, Kitami Institute of Technology, 165 Koen-cho, Kitami 090-8507, Japan

Abstract

A blind deconvolution method is developed on conditions: a point spread function is band-limited, both an object and a PSF are nonnegative, and output is a diffraction-limited object. These conditions enables the development of a practical blind deconvolution method cooperating with nonnegativity constraint. Computer simulations conducted to investigate the performance of the method.

OCIS codes

Blind deconvolution (BD) is a problem of finding two unknown functions from their convolution[1]. As the two unknown functions, we can regard the intensity distribution of an object (object function) and a point spread function (PSF) in typical applications in Optics. A convolution image is then supposed to be observed through an optical system.

As known well, there is a condition under which BD is possible [2]: the supports of both an object and a PSF are exactly specified. This condition will be, however, seldom satisfied because the PSF of an optical system is usually band-limited and its extent is not finite. Thus, constraining a PSF with a finite support undesirably causes truncation at its edge. Moreover, even the support of an object is unknown in many cases when the object is to be unknown. In this Letter, we purpose to develop a practical BD method under three conditions: (a) a PSF is band-limited, (b) both an object and a PSF are nonnegative, and (c) an output from BD is not an object itself but its diffraction-limited version. We should emphasize to use no support constraint.

Condition (a) is indispensable to make BD practicable, as described above. We suppose that the spatial frequency spectrum of a PSF is zero beyond a cutoff frequency.

Condition (b) is always satisfied when using an incoherent imaging system because both an object function and a PSF have nonnegative intensity distribution. Nonnegativity of functions sometime plays an important role in BD[1,3,4]. The reason is, however, not yet clear why nonnegativity constraint is effective. In this Letter, we implement nonnegativity constraint as the way described by Biraud[4], which is followed by some authors[5-7]. We will illustrate the effect of such nonnegativity constraint.

Condition (c) is closely related to (a). Since an observed image is band-limited according to condition (a), we must estimate values of spatial frequencies outside of a cutoff frequency if we attempt to obtain an object itself. This indicates that BD algorithm must include

superresolution effect. We think supreresolution to be a difficult problem and believe that avoiding it will be advantageous in developing a BD method. In other words, condition (c) makes our problem easier. It is the first time to clearly treat condition (c) in BD problems, to our knowledge.

Now, we state our BD problem. We observe an object $o(x,y)$ through an incoherent optical system with a shift-invariant PSF $p(x,y)$, and then obtain a convolution image:

$$i(x,y) = o(x,y) * p(x,y), \tag{1}$$

where * denotes a convolution operation. Introducing an Airy Disk $m(x,y)$ with the same cutoff frequency as the PSF, we take its convolution with $i(x,y)$:

$$\begin{aligned} g(x,y) &= i(x,y) * m(x,y) \\ &= d(x,y) * p(x,y), \end{aligned} \tag{2}$$

where $d(x,y)$ is the diffraction-limited object defined by

$$d(x,y) = o(x,y) * m(x,y). \tag{3}$$

The resultant image $g(x,y)$ can be regarded as the convolution of $d(x,y)$ and $p(x,y)$. The BD problem considered here is then to obtain $d(x,y)$ and $p(x,y)$ from $g(x,y)$.

We next introduce nonnegativity constraint into our BD problem. A PSF $p(x,y)$ is supposed to be nonnegative, and $d(x,y)$ is also nonnegative because it is a convolution of two nonnegative functions. Therefore, we represent $p(x,y)$ and $d(x,y)$ as the squares of real functions $\phi(x,y)$ and $\psi(x,y)$ as

$$d(x,y) = \{\phi(x,y)\}^2 \tag{4}$$

and

$$p(x,y) = \{\psi(x,y)\}^2 , \tag{5}$$

respectively[4-7]. As a result, $g(x,y)$ becomes

$$g(x,y) = \{\phi(x,y)\}^2 * \{\psi(x,y)\}^2 \ . \tag{6}$$

Taking Fourier transform leads to

$$G(u,v) = \{\Phi(u,v) * \Phi(u,v)\}\{\Psi(u,v) * \Psi(u,v)\}, \tag{7}$$

where (u,v) is spatial frequency coordinates and uppercase functions denote the Fourier transforms of corresponding lowercase ones. This equation indicates that $G(u,v)$ is the product of two autoconvolutions of $\Phi(u,v)$ and of $\Psi(u,v)$. We can translate our BD problem as to obtain $\Phi(u,v)$ and $\Psi(u,v)$ from $G(u,v)$.

Let us consider the effect of nonnegativity constraint in Eq. (6). If we do not use the nonnegativity constraint, a BD problem is then conventional, that is to say, to solve $G(u,v)=D(u,v)P(u,v)$. For digital images, $G(u,v)$, $D(u,v)$ and $P(u,v)$ are specified with the values of pixels inside an same cutoff frequency. Thus, the numbers of such pixels in their spectra, N_G, N_D and N_P, are identical. In this case, BD problem means to solve a set of undetermined equations because the number of unknowns, (N_G+N_D), is always larger than that of equations, N_P. The introduction of nonnegativity constraint drastically improves situation. Since an autoconvolution operation enlarges a cutoff frequency twice, the areas of $\Phi(u,v)$ and $\Psi(u,v)$ are the quarter of those of $D(u,v)$ and $P(u,v)$, respectively (Fig. 1). As a result, the number of unknowns becomes $(N_G+N_D)/4$ that is less than N_P. Nonnegativity constraint favorably manages to change a problem of solving undetermined equations to that of solving overdetermined ones. A standard approach to solving overdetermined equations is to use least square minimization. We also use conjugate gradient minimization as frequently used in BD methods[1-7].

We now present our BD method. We define an error metric by

$$E = \sum_u \sum_v \left| G(u,v) - \{\Phi(u,v) * \Phi(u,v)\}\{\Psi(u,v) * \Psi(u,v)\} \right|^2 . \tag{8}$$

Minimizing this error metric with a conjugate gradient procedure[7], we estimate $\Phi(u,v)$ and $\Psi(u,v)$. Fourier-transforming them and successively taking squares, we can finally obtain estimates of $d(x,y)$ and $p(x,y)$. In the conjugate gradient minimization, the algorithm starts from initial estimates of $\Phi(u,v)$ and $\Psi(u,v)$, and alternatively renews them so as to reduce the error metric (Fig. 2). The iteration is terminated when the error decreases no more.

A key factor in driving our method is how to determine initial estimates. An intuitive procedure is to generate random numbers inside a cutoff frequency on both real and imaginary parts of $\Phi(u,v)$ and $\Psi(u,v)$, and then to force the real and imaginary parts to be even and odd, respectively. If we have some information on an object, a PSF or both, the following method will be advantageous: we first give initial estimates of $d(x,y)$ and $p(x,y)$ and then take squared roots of them to obtain $\phi(x,y)$ and $\psi(x,y)$. Although we must give the signs of pixel values in $\phi(x,y)$ and $\psi(x,y)$, we can not usually determine those. A rude but simple countermeasure is to set all the signs to be positive. Once we obtain $\phi(x,y)$ and $\psi(x,y)$, we take their Fourier transforms and then force resultant functions to be zero outside of a cutoff frequency to obtain $\Phi(u,v)$ and $\Psi(u,v)$. Such initial estimates will contain some information on $d(x,y)$ and $p(x,y)$. However, we should note that $d(x,y)$ and $p(x,y)$ inversely calculated from the initial estimates differ from those given. We will use the latter method in our simulation.

We have to comment about solutions obtained with our method. We expect to obtain the pair of $D(u,v)$ and $P(u,v)$ from the Fourier transform of Eq. (2):

$$\begin{aligned} G(u,v) &= I(u,v)M(u,v) = D(u,v)P(u,v) \\ &= O(u,v)M(u,v)P(u,v). \end{aligned} \tag{9}$$

There are, however, possible combinations of functions: (i) $D(u,v)$ and $P(u,v)$, (ii) $I(u,v)$ and $M(u,v)$, (iii) $O(u,v)\Pi(\underline{u},v)$ and $P(u,v)M(u,v)$, and (iv) $G(u,v)$ and $\Pi(u,v)$, where $\Pi(u,v)$ is a circle

function with the same cutoff frequency as $P(\underline{u},v)$. The circle function is necessary because our algorithm restricts frequency region to be recovered inside a cutoff frequency. Combination (i) is the solution we want. Combination (ii), which is of an observed image itself and an Airy disk, is known as a trivial solution. Combinations (iii) and (iv) never appear as a solution of our BD problem, since they break nonnegativity constraint. The breakage of nonnegativity is because the Fourier transform of $\Pi(u,\underline{v})$ contains negative pixel values. We can regard that explicit solutions with our method are only those of combinations (i) and (ii).

We now demonstrate our method with computer simulations. We used a two-point object with the intensity ratio of 0.6, which is shown in Fig. 3(a), and stellar speckle-like PSF. Figure 3(b) shows their convolution image with noise of 25 dB. As initial estimates of $d(x,y)$ and $p(x,y)$, we adopt random-valued disks with the radius of 10 pixels. Image size is with 64x64 pixels. Figure 3(c) shows an image obtained with our method. We can clearly see two points in the image. Its mean square error to the original object (Fig. 3(a)) was 0.056. For comparison, we show an image obtained with the method by Ayers and Dainty in Fig. 3(d). Its MSE was 0.692.

Through the following simulation, we describe the dependency of solutions on initial estimates. We fixed the initial estimate of PSF to be a random-valued disk with the radius of 30 pixels, and used two points with a variable intensity ratio as the initial estimate of an object. We conducted our BD method with changing the intensity ratio from 0.0 to 1.0 with the interval of 0.1, and then measured the intensity ratio of resultant two points.

Figure 4 shows the result. In the graph, the horizontal axis is the intensity ratio of an initial estimate. The vertical axes show the intensity ratio of resultant two points (solid squares) and an error value E with which the algorithm converged (open circles). When the intensity ratio of an initial estimate was zero, both the resultant intensity ratio and the error value were zero.

This case corresponds to the trivial solution. In the two cases with initial intensity ratios of 0.1 and 0.2, BD failed so that the resultant intensity ratios seriously deviated from the true value 0.6 and the error values became larger than the others. For intensity ratios of initial estimates larger than 0.2, resultant intensity ratios were near to 0.6. In addition, error values were almost same. From these results, we judged that the algorithm converged near to the true solution.

In Fig. 4, we can see that a valley of error values around the trivial solution will be deep and narrow. On the other hand, a valley around the true solution will be relatively shallow but broad. In our simulations, the trivial solution occurred only from the initial estimate with the intensity ratio of 0.0. At least, we can say that the trivial solution seldom occurs from initial estimates other than itself.

In conclusion, we treated the fore-mentioned conditions (a), (b) and (c) in BD problems for the first time, to our knowledge, and then proposed a BD method. The method is practical in applications in Optics because of the adoption of the conditions. We also described that the introduction of nonnegativity constraint leads a BD problem of solving a set of overdetermined equations, which will be not unsolvable. We demonstrated the performance of our method through simulations. Our method can produce not only a true solution but also a trivial solution. However, we showed that a trivial solution would have less feasibility.

References

1. G. R. Ayers and J. C. Dainty, Opt. Lett., 13 (1988) 547.
2. R. G. Lane and R. H. T. Bates, J. Opt. Soc. Am. A, 4 (1987) 180.
3. R. G. Lane, J. Opt. Soc. Am. A, 9 (1992) 1508.
4. E. Thiebaut and J.-M. Conan, J. Opt. Soc. Am. A, 12 (1995) 485.
5. Y. Biraud, Astron. AstroPhys., 1 (1969) 124.
6. N. Miura and N. Baba, Opt. Lett., 21 (1996) 1174.
7. N. Miura and K. Kikuchi, Proc. of the SPIE, 4829 (2002) 213.
8. W. H. Press, B. P. Flannery, S. A. Teukolsky, and W. T. Vetterling, Numerical Recipes in C (Cambridge U. Press, Cambridge, 1988)

Figure captions

Fig. 1. Illustration of effectiveness on nonnegativity constraint.

Fig. 2. Proposed method.

Fig. 3. Demonstration with simulation: (a) object, (b) noisy convolution image, (c) image restored with the present method, and (d) image obtained with the Ayeres-Dainty method.

Fig. 4. Dependence on initial estimate.

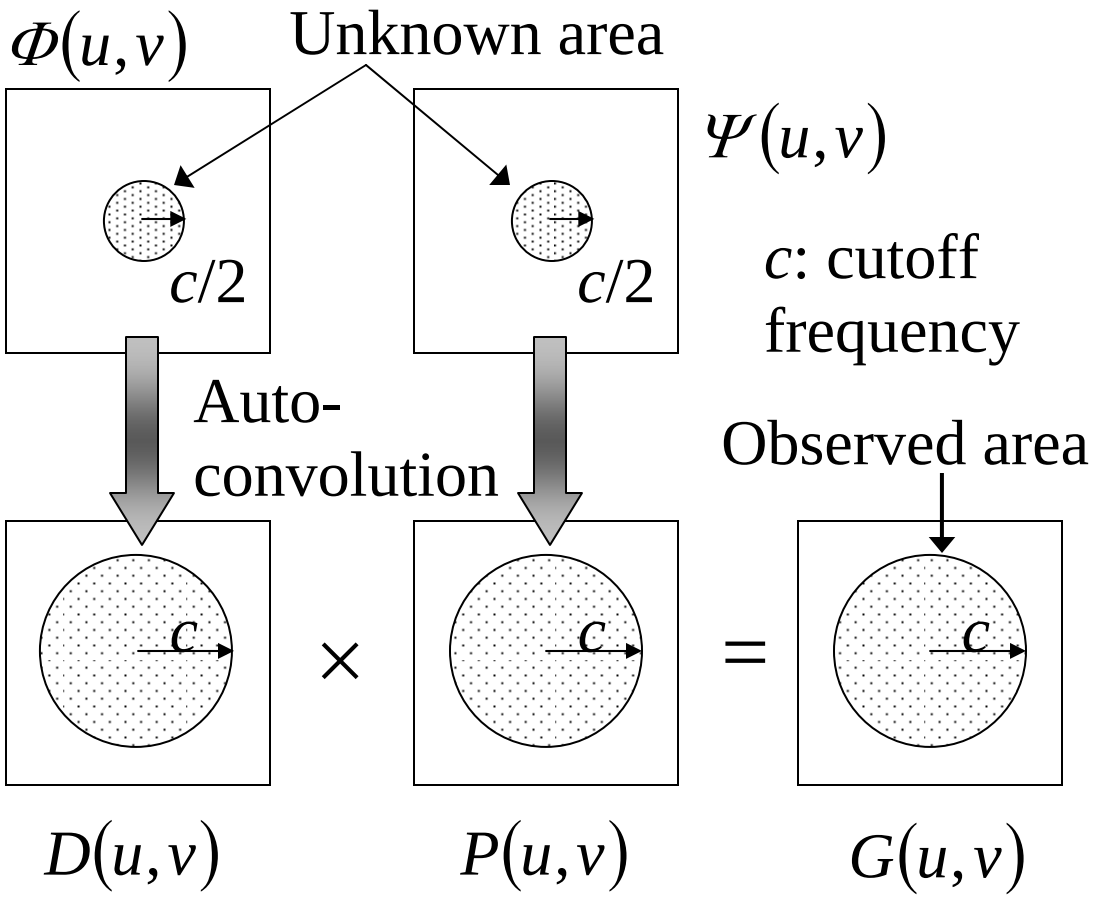
$\Phi(u,v)$
Unknown area
$\Psi(u,v)$
$c/2$
$c/2$
c: cutoff frequency
Auto-convolution
Observed area
c
$\times$
c
$=$
c
$D(u,v)$
$P(u,v)$
$G(u,v)$

Fig. 1

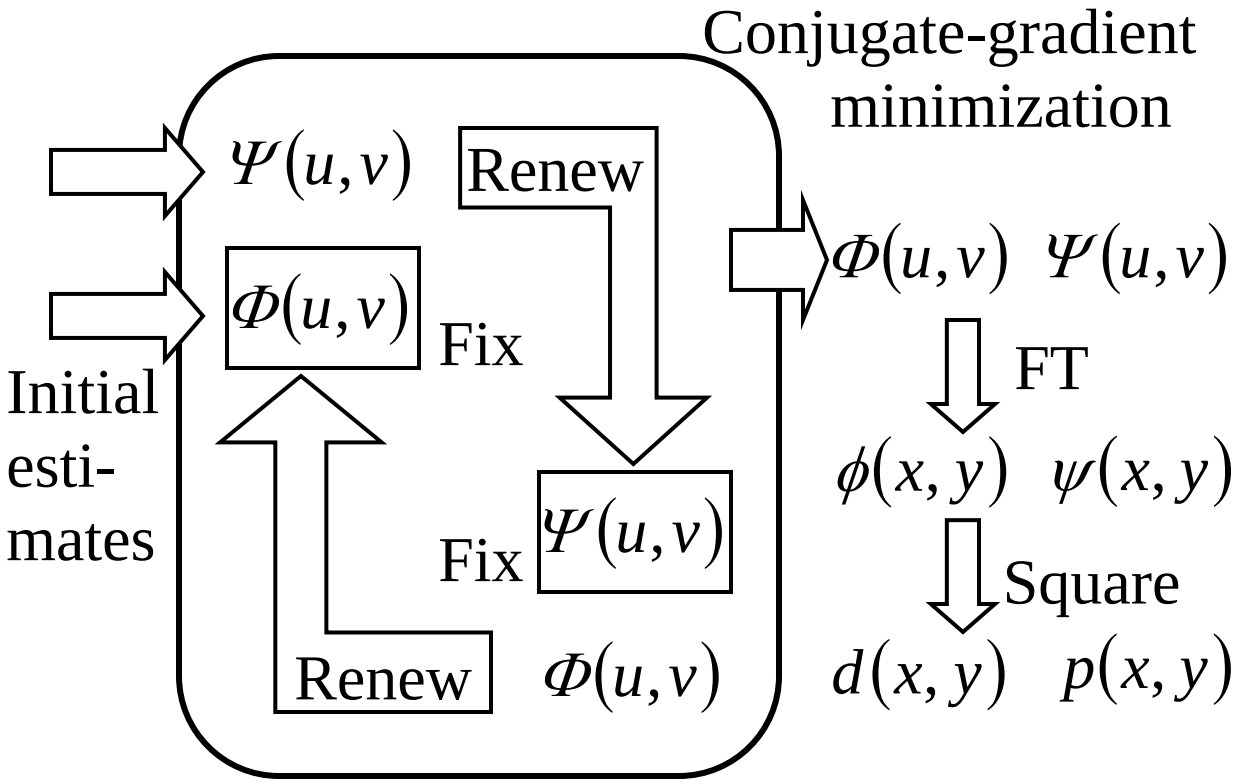
Conjugate-gradient
minimization
$\Psi(u,v)$
Renew
$\Phi(u,v)$
Fix
Initial
esti-
mates
Fix
$\Psi(u,v)$
Renew
$\Phi(u,v)$
$\Phi(u,v)$ $\Psi(u,v)$
FT
$\phi(x,y)$ $\psi(x,y)$
Square
$d(x,y)$ $p(x,y)$

Fig. 2

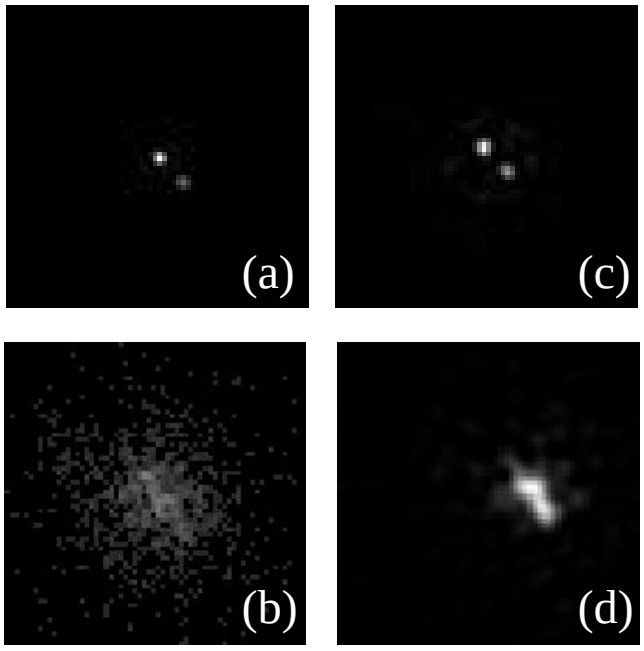

Fig.3

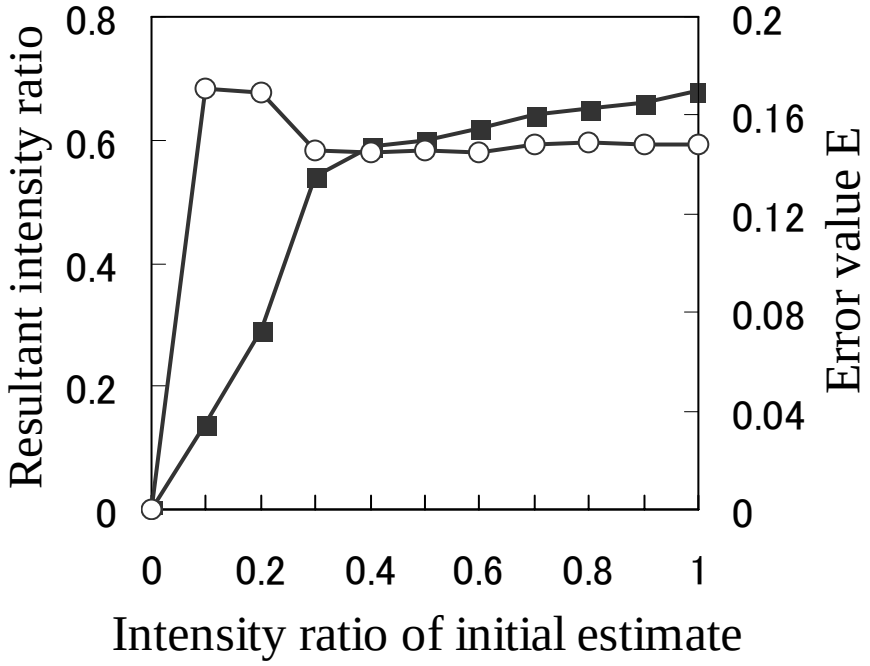
Resultant intensity ratio
0.8
0.6
0.4
0.2
0
0.2
0.16
0.12
0.08
0.04
0
Error value E
0
0.2
0.4
0.6
0.8
1
Intensity ratio of initial estimate

Fig. 4